Asian Journal of Chemistry; Vol. 32, No. 12 (2020), 3035-3042

ASIAN JOURNAL OF CHEMISTRY

https://doi.org/10.14233/ajchem.2020.22888

Hydrolytic Degradation Study of Rivaroxaban: Degradant Products Identification by LC-MS Isolation by Prep-HPLC and Characterization by HRMS, NMR and FT-IR

G. Mahesh Kumar Reddy[1,2], Raghu Babu Korupolu[2], B. Kishore Babu[2], J.C.M.K.N.N. Murty Singamsetti[1], Chidananda Swamy Rumalla[1,*], Muralidharan Kaliyaperumal[1], Raju Doddipalla[1] and Rajani Vijay[1]

[1]Department of Medicinal Chemistry, GVK Biosciences Pvt. Ltd., IDA Nacharam, Hyderabad-500076, India
[2]Department of Engineering Chemistry, Andhra University, Visakhapatnam-530003, India

*Corresponding author: E-mail: rchidanandaswamy@gmail.com

Received: 6 July 2020; *Accepted*: 5 September 2020; *Published online*: 7 December 2020; AJC-20136

Present work illustrates the stress degradation behaviour of rivaroxaban under hydrolytic, oxidative, thermal and photolytic conditions as per ICH guidelines. Under thermal and photolytic conditions drug had a fair stability where as in other stress conditions degradation products were observed. Initial identification of the degradation products was performed by hyphenated mass spectrometry coupled to ultra-performance liquid chromatography (UPLC-MS) and mass directed auto purification (MDAP) was used for isolation. Various 1D and 2D nuclear magnetic resonance (NMR) were performed to characterize the degradation products which were assisted by FT-IR and HRMS data. Two novel degradant products were observed in hydrolytic conditions, isolated and characterized by spectroscopic techniques as (*R*)-2-(2-((4-((3-(5-chlorothiophene-2-carboxamido)-2-hydroxypropyl)amino)phenyl)amino)ethoxy)acetic acid (**DP-2**) (*m.w.* of 427.90 g/mol and *m.f.* $C_{18}H_{22}N_3O_5SCl$), and 5-chlorothiophene-2-carboxylic acid (**DP-3**) (*m.w.* 161.95 g/mol and *m.f.* $C_5H_3O_2SCl$). Additionally, two more degradation products were observed in basic and acidic conditions, *viz*. (*R*)-5-chloro-*N*-(2-hydroxy-3-((4-(3-oxomorpholino)-phenyl)amino)propyl)thiophene-2-carboxamide (**DP-1**) (*m.w.* 409.09 g/mol and *m.f.* $C_{18}H_{20}N_3O_4SCl$) and (*S*)-2-(2-((4-(5-((5-chlorothiophene-2-carboxamido)methyl)-2-oxooxazolidin-3-yl)phenyl)amino)ethoxy)acetic acid (**DP-4**) (*m.w.* 453.08g /mol and *m.f.* $C_{19}H_{20}N_3O_6SCl$) are already reported.

Keywords: Rivaroxaban, Forced Degradation, HRMS.

INTRODUCTION

Rivaroxaban is a recently developed first and only oral anti-coagulant and direct factor Xa inhibitor, which is used in the prevention of stroke and venous embolism in patients with chronic atrial fibrillation, as well as treatment and prevention of deep venous thrombosis (DVT) and pulmonary embolism. Deep venous thrombosis (DVT) prophylaxis after knee or hip replacement surgery, reduces the risk of recurrence and stroke in patients with non-valvular atrial fibrillation [1-6].

Rivaroxaban (m.f. $C_{19}H_{18}N_3O_3SCl$ and m.w. 435.88 g/mol) chemically known as (*S*)-5-chloro-*N*-((2-oxo-3-(4-(3-oxomorpholino)phenyl)oxazolidin-5-yl)methyl)thiophene-2-carboxamide is an oral anticoagulant invented and manufactured by Bayer [7-11]. Rivaroxaban, sold under the brand name Xarelto among others, is an anticoagulant medication (blood thinner) used to treat and prevent blood clots. Specifically, it is used to treat deep vein thrombosis and pulmonary emboli and prevent blood clots in atrial fibrillation and following hip or knee surgery [12-14]. It works by blocking the activity of the clotting protein factor Xa. Rivaroxaban was patented in 2007 and approved for medical use in the United States in 2011. In United States, it will not be available as a generic medication until 2024. Rivaroxaban was the 105th most prescribed medication in the United States with more than 7 million prescriptions [15,16].

An extensive literature survey reveals that there were few analytical methods available for the determination of rivaroxaban in plasma, biological fluids, bulk and in pharmaceutical dosage forms by liquid chromatography (HPLC) and liquid chromatography mass spectrometry (LC-MS) techniques [17-21]. But none of the literature methods mentioned about the identi-fication and characterization of degradation products formed under different stress conditions and possible process related impurities of rivaroxaban in bulk drugs [22-25]. As per the ICH and other guidelines, the pharmaceutical importance of drugs has prompted us to carry out a detailed

study using various instruments like LCMS, Prep-HPLC, HRMS, NMR and FT-IR on identification, and characterization of degradation products of rivaroxaban.

EXPERIMENTAL

Rivaroxaban was received as a gift sample from a reputed manufacturing unit in Hyderabad, India. High purity ultra-pure water was obtained by using a Millipore Milli-Q water purification system. HPLC grade acetonitrile and methanol were purchased from Merck, Germany. Analytical grade trifluoroacetic acid, HCl, H_2O_2 (30% w/w) and NaOH were purchased from Sigma-Aldrich Chemicals Pvt. Ltd., India.

Ultra performance liquid chromatography-mass spectrometry (UPLC-MS): A prominence series Waters Acquity UPLC system equipped with a binary solvent manager pump, an auto sampler, and PDA detector with empower-3 software was used for method development, validation and stress degradation studies. The chromatographic column used was Acquity; UPLC; BEH-C18 column [(100 × 2.1) mm; 1.7 µm], which was procured from WATERS. The mobile phase components are A: 0.1% formic acid (Aq), B: acetonitrile, separation was accomplished in a gradient elution program {time (min)/% B: 0.0/10, 4/98, 4.1/10, 6/10} at a flow rate of 0.5 mL/ min. The chromatographic eluents were monitored at a detection wavelength of 215 nm using a photodiode array (PDA) detector, the injection volume of 1.0 µL was used for sample injections. Water and acetonitrile in the ratio of 50:50(v/v) was used as diluent.

Waters SQ Detector-2 single quadrupole mass spectrometer operated in dual polarity-positive and negative with electrospray ionization source (ESI) was used for mass spectral analysis. Full scan mode 100-1500 Daltons (Da) was used for the MS optimization. The capillary voltage and source temperature were set to 3.5 kV and 140 ºC, respectively. The desolvation temperature was set at 350 ºC. The desolvation gas flow was set at 650 L/h, while the cone gas flow was set at 50 L/h. The LC instrument and the mass spectrometer were controlled by Masslynx 4.1 Application Manager. The injection volume was 1.0 µL with sample manager temperature maintained at 10 ºC and the chromatographic runtime of 7.0 min.

High resolution mass spectrometry (HRMS): Isolated impurities were analyzed on Thermo scientific Q-exactive orbitrap HRMS instrument with ESI ion source. The front end inlet used was UHPLC Dionex Ultimate 3000 instrument which comprises of binary pump, column manager and PDA detector. The mass parameters were optimized as follows: Capillary voltage: 3500 V; Sample cone voltage: 30 V; Extraction cone voltage: 5 V; Source temperature: 140 ºC; Desolvation temperature: 300 ºC; Cone gas: 50 L/h; Desolvation gas: 650 L/h. Sample was analyzed in positive mode and negative mode and data was acquired using X-Caliber software. MS/MS analysis was performed to identify the fragmentation patterns using the collision energy of 35 eV. Acquity; BEH; C18, 50 × 2.1 mm, 1.7 µ particle size column was used with flow rate: 0.6 mL/ min and mobile phase of 0.1% formic acid in water and acetonitrile is used in gradient mode.

Mass mediated preparative HPLC: The forced degradation sample was purified on Waters preparative HPLC equipped with 2545 pump module, 2998 PDA detector Acquity QDA mass detector module 3100 and 2707 sample manager with auto fraction collector. Mass lynx software was used to monitor the purification run. Preparative column used was X-Bridge shield RP-18; 250 ×19 mm; 5 µ with a flow rate of 20 mL/min. Mobile phase used was 0.1% v/v formic acid in aqueous and acetonitrile. Mass capillary voltage was maintained at 3.0 kV, Source temperature 150 ºC and desolvation temperature at 350 ºC. The desolvation gas flow was set at 650 L/h. The cone gas flow was set at 50 L/h. Ammonium acetate (20mM) and acetonitrile (30: 70, v/v) were used as a makeup solvent with makeup flow of 0.3 mL/ min to the mass detector and 1:1000 splitting ratio was maintained for the proper ionization.

NMR spectroscopy: The ^1H, ^{13}C NMR and 2D NMR spectra of Tavaborole API and degradation impurity were recorded in DMSO-d_6 solvent on Agilent MR400MHz NMR instrument equipped with 5 mm ONE NMR probe with Z-gradient shim system which has the sensitivities of 480:1 and 225:1. The ^1H NMR spectra were referenced to tetramethyl silane (TMS) singlet at zero (0) ppm and referenced DMSO-d_6 septet at 39.5 ppm in ^{13}C NMR spectrum. ^1H NMR data acquired and processed with following parameters spectral width (SW) = 17.95 ppm, relaxation delay time (D1) = 1 s, 900 pulse width (PW90) = 7.4 µs, acquisition time (AT) = 4.0 s, operating spectrometer frequency (SF) = 399.63 MHz. The ^{13}C NMR data acquired and processed with following parameters spectra width (SW) = 248.8 ppm, relaxation delay (D1) = 3 s, 900 pulse width (PW90) = 7.6 µs, acquisition time (AT) = 1.31 s and spectrometer frequency (SF) = 100.48 MHz parameters.

The 2D 1H-1H gDQCOSY experiment has been performed to know the proton-proton correlations with following parameters, gHSQC was done to know the ^1J correlations between proton-carbon with and gHMBC has been performed to identify the ^3J correlations and reveal the exact structure of degradation product

FT-IR analysis: The FT-IR was used to obtain the information about various functional groups present in the degradation products. Perkin-Elmer spectrum 100 model was used with KBr as dispersion medium to make the sample pellets.

Sample preparation

Forced degradation: As per ICH stability guidelines [26-29], various stress parameters *i.e.* acidic, basic, oxidation, thermal and photolytic conditions were employed.

Preparation of degradation samples for purification: Degradation was observed in acidic and basic conditions. Acid degraded sample was neutralized with saturated solution of ammonium bicarbonate and resultant solution was lyophilized to get crude solid sample. The same was dissolved in 4-5 mL of mobile phase (50:50; H_2O:CH_3CN). For base degradation, degraded sample was neutralized with 5N HCl solution and the resultant solution was evaporated to get free solid and same sample was dissolved in 4-5 mL of mobile phase for HPLC purification.

Degradation behaviour of rivaroxaban: Rivaroxaban drug substance did not show any degradation under heating (60 ºC), UV(λ = 254 nm), The drug was found to be labile to acid hydrolysis as a total of 44.2% degradation was found

(1N HCl refluxed at 60 ºC, up to 10 h) with **DP-3** 1.90% and **DP-4** 39.26%. The drug degradation was also found in base degradation of 38.93% (0.1 N NaOH kept at room temperature up to 10 h) with an individual **DP-1** of 10.67% and **DP-3** of 22.88%. Additionally, in oxidative degradation 4.27% (10% H_2O_2 refluxed at 60 ºC up to 48 h) with DP-2 of 4.18% was observed. Degradation details are shown in Table-1. The acid, base, oxidative, thermal and photolytic degradation chromatograms are shown in Fig. 1.

RESULTS AND DISCUSSION

The degradants were formed after specific time and after each stress study conditions as mentioned in the experimental section. To determine the results of the solutions from all the stress studies, samples were analyzed individually using mass spectrometry. Three significant degradation products formed in the study were isolated, identified and characterized by LCMS, HRMS, NMR (1D and 2D) and FT-IR techniques.

Isolation of degradation products: The degradation was observed in acidic and basic stress conditions with adequate percentage formation of > 5%. Purification was carried out using 0.1% formic acid (aq) and acetonitrile as a mobile phase with Kromasil C18 column with dimensions (150 mm × 25 mm) 10 µ. Crude sample solutions were injected in consecutive injections and the fractions were collected on the basis of mass threshold parameters of total ion chromatogram. After completion of the degradation procedure, the degradants were purified in mass pre-mediated HPLC to collect all the fractions pertaining to molecular weight of 160.95 (M-H), 454.18 (M+H) pooled separately and lyophilized to get free solid. In base degradation, fractions of mass 410.09 (M+H) and 428.90 (M+H) pooled separately together and lyophilized to get free solid.

Characterization of degradation product-1 (DP-1): To get structural informations, HRMS analysis of **DP-1** performed and got the protonated molecular ion $(M+H)^+$ as a value of 408.0786 (M-H) with 1.522 ppm error for the calculated molecular formula of $C_{18}H_{19}N_3O_4SCl$ (Fig. 2b). To know more insights of the impurity, full characterization has been done by NMR 1D and 2D experiments. On comparing the NMR data of API and **DP-1**, two extra exchangeable protons, at 5.64 ppm and 5.10 ppm with multi-

TABLE-1
RIVAROXABAN FORCE DEGRADATION STUDIES

Conditions	DP-1	DP-2	DP-3	DP-4	API
Rivaroxaban API	–	–	–	–	99.64
Acid (1 N HCl reflux at 60 °C, 10 h)	–	–	1.90	39.26	55.80
Base (0.1 N NaOH RT up to 10 h)	10.67	22.88	–	1.93	61.07
Oxidation (10% H_2O_2 reflux at 60 °C, 48 h)	–	–	–	4.18	95.72
Thermal (exposure to 120 °C for 48 h)	–	–	–	0.74	98.75
Photolytic (exposed at 254 nm for 48 h)	–	–	–	–	99.61

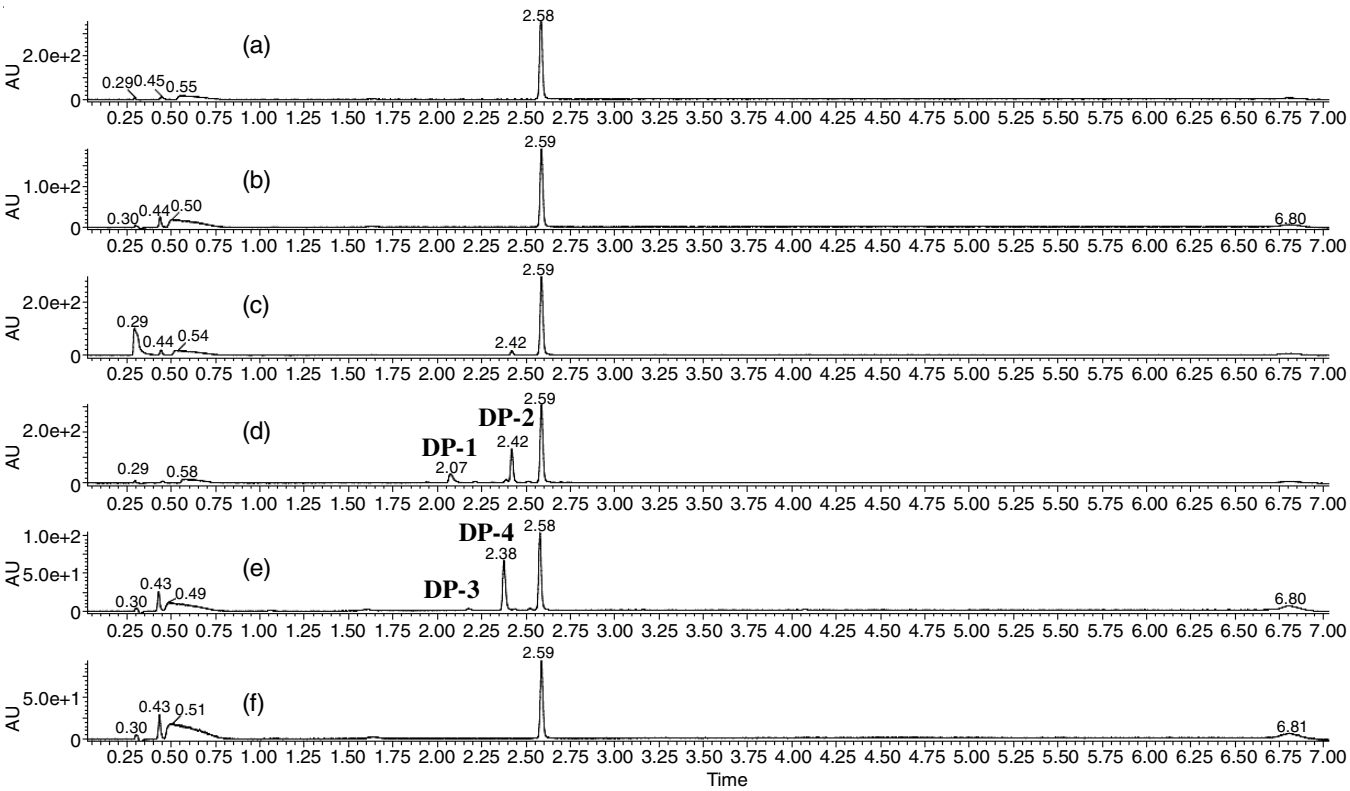

Fig. 1. LCMS chromatograms of rivaroxaban degradant products (a) photolytic degradation (b) thermal degradation (c) oxidative degradation, (d) alkaline degradation, (e) acid degradation and (f) rivaroxaban-API

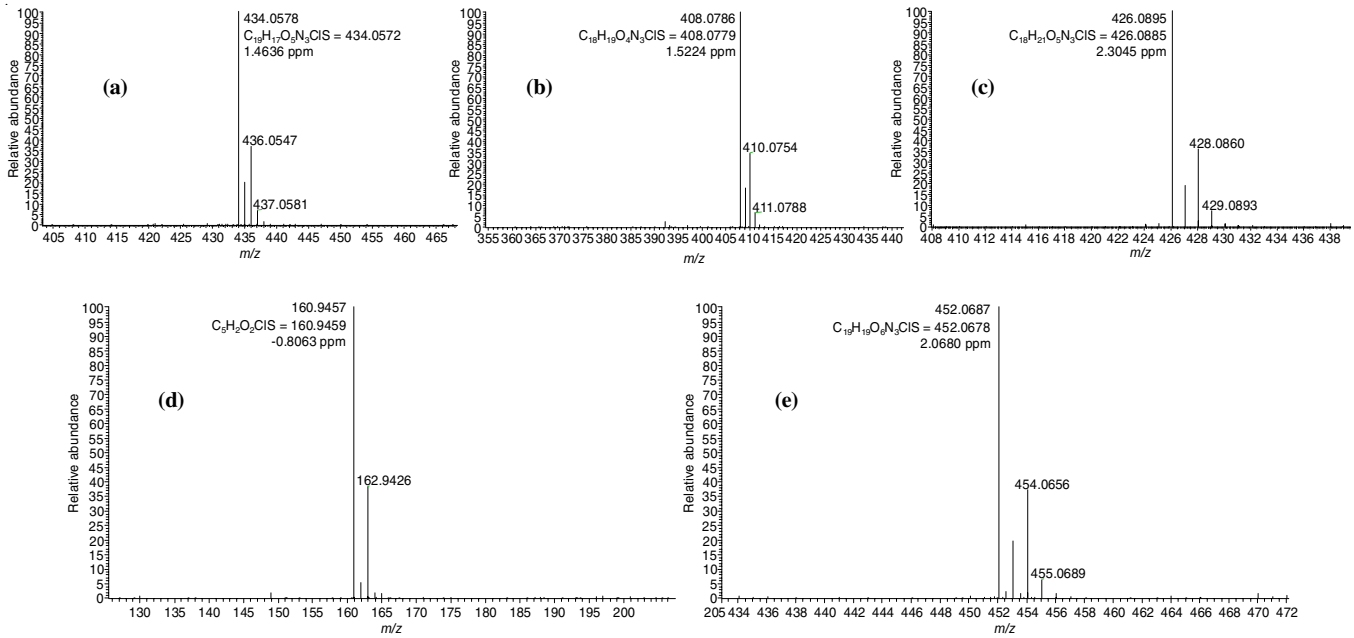

Fig. 2. HRMS chromatograms of rivaroxaban (a) API (b) **DP-1**, (c) **DP-2**, (d) **DP-3**, (e) **DP-4**

plicity triplet and broad singlet, respectively were observed. In ^{13}C NMR, the total accountability of the carbon signals is equal to 18 instead of 19 (API), which indicates that one of the carbons is missing. The overlain carbon spectrum implies that the signal at 154.08 ppm was absent and is further confirmed by ^{1}H-^{13}C HMBC experiment. In HMBC data the triplet at 5.64 ppm shows correlation to C9 & 11 protonated carbon at 111.91 ppm. Presence of two extra exchangeable protons and missing carbonyl carbon supported the assumption of the carbamate ring opening by the elimination of carbonyl group. Based on these key points, the confirmed structure is shown in Fig. 3.

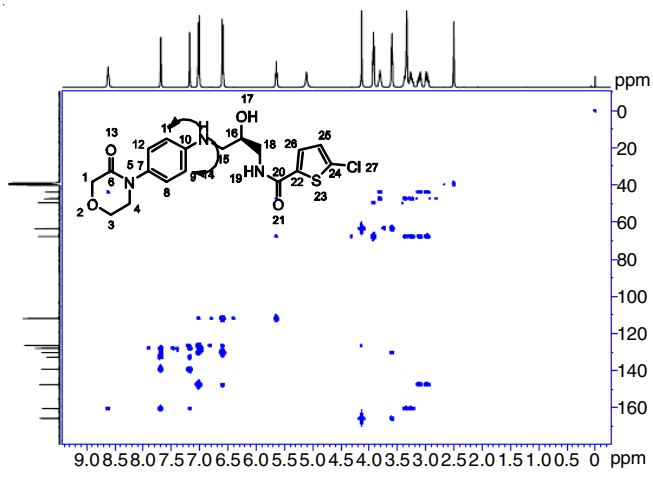

Fig. 3. NMR-HMBC spectra of rivaroxaban **DP-1**

Further, stretching frequency at 3386 and 3332 cm^{-1} in FTIR spectra indicates the presence of OH and NH groups, stretching frequency at 1745, 1717 and 1633 cm^{-1} indicates the presence of keto and amide group and stretching frequency at 813 and 754 cm^{-1} indicates the presence of chloro and sulphur groups, respectively. From FT-IR, major frequencies confirmed the presence of sulphur, alcohol, amide, amine and keto functional groups as shown in Table-2. A possible mechanism of **DP-1** formation from API by base degradation is shown in Fig. 4.

Degradation product-2: The HRMS data of **DP-2** was found to be 426.0895 (M-H) with 2.3045 ppm error for the calculated molecular formula of $C_{18}H_{21}N_3O_5SCl$ as shown in Fig. 2c. To elucidate the structure ^{1}H & ^{13}C NMR, HMBC, HSQC and FT-IR data were recorded. The NMR chemical shifts of **DP-2** are given in Table-2. The proton NMR of **DP-2** shows a significant change in the chemical shift of 3-morpholinone ring. The chemical shift of methylene group (-CH_2-) has shifted 0.7 ppm upfield from 3.71 ppm to 3.05 ppm and also in carbon NMR the same methylene carbon has shifted up field ~5.0 ppm from 48.99 ppm to 44.16 ppm. The amidic carbonyl carbon of 3-morpholinone ring shifted downfield nearly 6.6 ppm from 165.94 ppm to 172.6 ppm, and in HMBC data, there is no correlation of methylene group (-CH_2-) protons with the same amidic carbonyl carbon (C_6). This specifies that 3-morpholinone ring got opened and substituted 2-(2-aminoethoxy)acetic acid has formed as shown in Fig. 5.

In ^{13}C NMR the number of carbons were 18 whereas 19 in API, which indicates that one of the carbon was missing. The carbon at 154.08 ppm in API was not seen in **DP-2** ^{13}C NMR. In ^{1}H-^{13}C HMBC, at aromatic region the carbamate ring methylene group protons (-CH_2-) shows ^{3}J correlation with only C_{10} carbon at 140.28 ppm and no other correlation was noticed especially above 145 ppm. This key point disclosed the ring opening of carbamate ring by loss of carbonyl group. All the exchangeable protons (indicated with colour differentiation in Fig. 5) excluding amidic –NH undergone chemical exchange with DMSO-d_6 moisture and observed as a broad hump at 4 to 5 ppm region in proton NMR. In FTIR, stretching frequency at 3359 cm^{-1} with broad signal indicates the presence of acid group, stretching frequency at 1735 and 1644 cm^{-1}

TABLE-2
COMPARATIVE NMR ASSIGNMENTS FOR RIVAROXABAN AND DEGRADATION PRODUCTS

Atom No.	Type of atom	^{1}H Chemical shift (ppm) coupling const (*J*)	^{13}C Chemical shift (ppm)	Type of atom	^{1}H Chemical shift (ppm) coupling const (*J*)	^{13}C Chemical shift (ppm)
		API			**DP-1**	
1	CH_2	4.19 (s, 2H)	67.71	CH_2	4.13 (s, 2H)	67.73
2	O	-	-	O	-	-
3	CH_2	3.97 (t, 5.2Hz, 2H)	63.45	CH_2	3.92 (t, 5.6Hz, 2H)	63.55
4	CH_2	3.71 (t, 5.2Hz, 2H)	48.99	CH_2	3.59 (t, 5.6Hz, 2H)	49.60
5	N	-	-	N	-	-
6	C	-	165.94	C	-	165.77
7	C	-	137.05	C	-	130.24
8	CH	7.41 (m, 2H)	125.93	CH	7.00 (d, 8.8Hz, 2H)	126.48
9	CH	7.55 (m, 2H)	118.32	CH	6.60 (d, 8.8Hz, 2H)	111.91
10	C	-	136.47	C	-	147.45
11	CH	7.55 (m, 2H)	118.32	CH	6.60 (d, 8.8Hz, 2H)	111.91
12	CH	7.41 (m, 2H)	125.93	CH	7.00 (d, 8.8Hz, 2H)	126.48
13	O	-	-	O	-	-
14	N	-	-	NH	5.64 (t, 6.0Hz, 1H)	-
15	CH_2	3.85 (dd, 9.2, 6.4Hz, 1H) 4.19 (t, 9.2Hz, 1H)	47.41	CH_2	2.97 (m, 1H) 3.10 (m, 1H)	47.38
16	CH	4.84 (m, 1H)	71.31	CH	3.80 (m, 1H)	67.77
17	O	-	-	OH	5.10 (broad singlet, 1H)	-
18	C	-	154.08	CH_2	3.26 (m, 1H) 3.33 (m, 1H)	43.86
19	O	-	-	NH	8.62 (broad triplet, 1H)	-
20	CH_2	3.60 (t, 5.6Hz, 2H)	42.19	C	-	160.36
21	NH	8.97 (t, 6.0Hz, 1H)	-	O	-	-
22	C	-	160.78	C	-	132.73
23	O	-	-	S	-	-
24	C	-	133.25	C	-	139.23
25	S	-	-	CH	7.17 (d, 4.0Hz, 1H)	127.95
26	C	-	138.44	CH	7.68 (d, 4.0Hz, 1H)	128.02
27	CH	7.19 (d, 4.0Hz, 1H)	128.13	Cl	-	-
28	CH	7.69 (d, 4.0Hz, 1H)	128.43			
29	Cl	-	-			
		DP-2			**DP-4**	
1	CH_2	3.85 (s, 2H)	68.88	CH_2	4.03 (s, 2H)	67.55
2	O	-	-	O	-	-
3	CH_2	3.57 (t, 5.6Hz, 2H)	69.28	CH_2	3.60 (t, 6.0Hz, 2H)	69.21
4	CH_2	3.05 (t, 5.6Hz, 2H)	44.16	CH_2	3.17 (t, 6.0Hz, 2H)	42.85
5	NH	-	-	NH	Broad hump	-
6	C	-	172.6	C	-	171.81
7	C	-	140.35	C	-	145.71
8	CH	6.44 (m, 2H)	113.79	CH	6.60 (d, 8.8Hz, 2H)	112.03
9	CH	6.45 (m, 2H)	113.96	CH	7.20 (d, 8.8Hz, 2H)	120.76
10	C	-	140.28	C	-	127.35
11	CH	6.45 (m, 2H)	113.96	CH	7.20 (d, 8.8Hz, 2H)	112.03
12	CH	6.44 (m, 2H)	113.79	CH	6.60 (d, 8.8Hz, 2H)	120.76
13	O	-	-	O	-	-
14	NH	Broad hump	-	N	-	-
15	CH_2	2.86 (dd, 12.4, 6.8Hz 1H) 3.00 (dd, 12.4, 4.8Hz 1H)	48.73	CH_2	3.73 (dd, 8.8, 6.0Hz 1H) 4.06 (t, 8.8Hz 1H)	48.16
16	CH	3.79 (m, 1H)	67.93	CH	4.75 (m, 1H)	70.96
17	OH	Broad hump	-	O	-	-
18	CH_2	3.24 (m, 1H) 3.34 (m, 1H)	43.98	C	-	154.38
19	NH	8.71 (t, 5.6Hz, 1H)	-	O	-	-
20	C	-	160.36	CH_2	3.56 (t, 5.6Hz, 2H)	42.29
21	O	-	-	NH	8.95 (t, 6.0Hz, 1H)	-
22	C	-	132.68	C	-	160.75
23	S	-	-	O	-	-
24	C	-	139.32	C	-	133.22
25	CH	7.17 (d, 4.0Hz, 1H)	127.99	S	-	-
26	CH	7.71 (d, 4.0Hz, 1H)	128.03	C	-	138.5
27	Cl	-	-	CH	7.21 (d, 4.0Hz, 1H)	128.14
28	OH	Broad hump	-	CH	7.69 (d, 4.0Hz, 1H)	128.4
29				Cl	-	-
				OH	Broad hump	-

s: singlet; d: doublet; m: multiplet; ss: singlet of singlet; dd: doublet of doublet; dm: double multiplet; bh: broad hump.

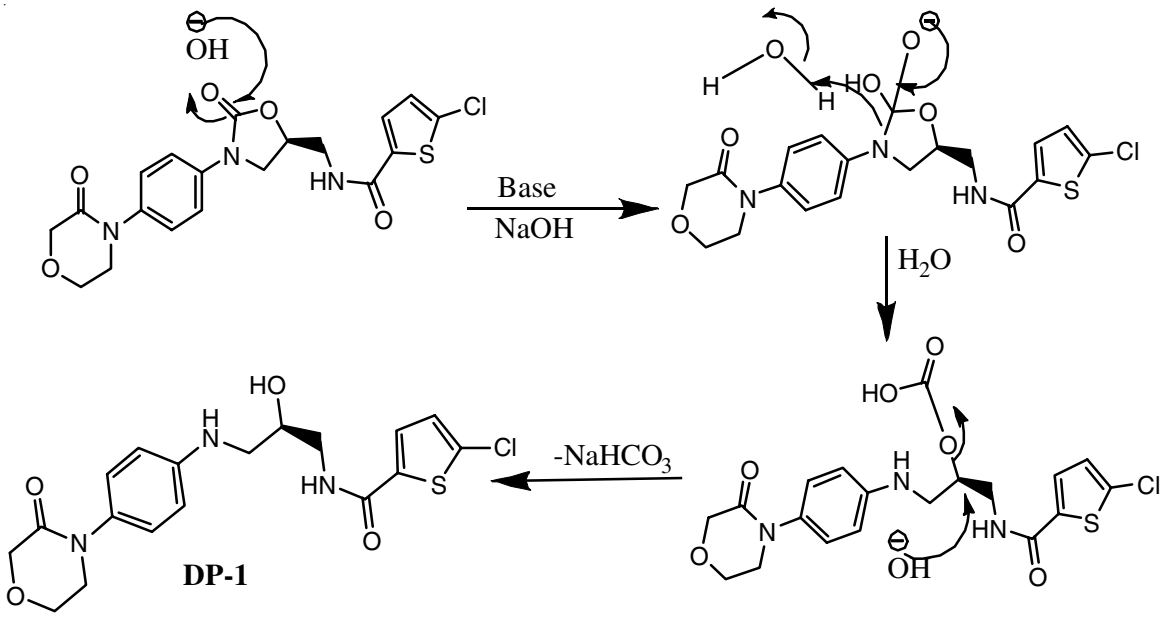

Fig. 4. Possible mechanism of **DP-1** formation

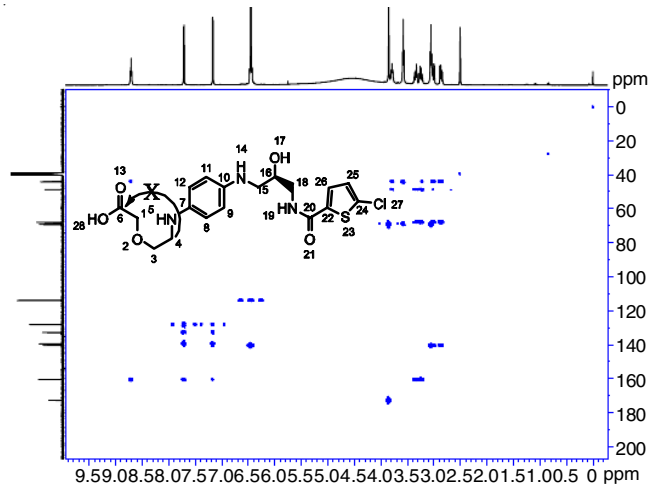

Fig. 5. NMR-HMBC spectra of rivaroxaban **DP-2**

indicates the presence of keto and amide group, stretching frequency at 814 and 740 cm^{-1} indicates the presence of chloro and sulphur group. From FT-IR, major frequencies confirmed the presence of acid, alcohol, amide, amine, sulphur and keto functional groups are summarized in Table-3. A possible mechanism of **DP-2** formation from API through base degradation is shown in Fig. 6.

Degradation product-3: The **DP-3** HRMS data showed the exact mass of 160.9457 (M-H) with -0.8063 ppm error for the calculated molecular formula of $C_5H_2O_2SCl$ as shown in Fig. 2d. The **DP-3** formation in base degradation is very low and difficult to isolate. Based on available quantity, the structure characterization has been carried out only based on proton NMR, HRMS and FT-IR. In ^1H NMR, only two aromatic protons were observed at 7.00 and 7.17 ppm with 4 Hz coupling constant (*J*). The FTIR stretching frequency at 3442 cm^{-1} with broad

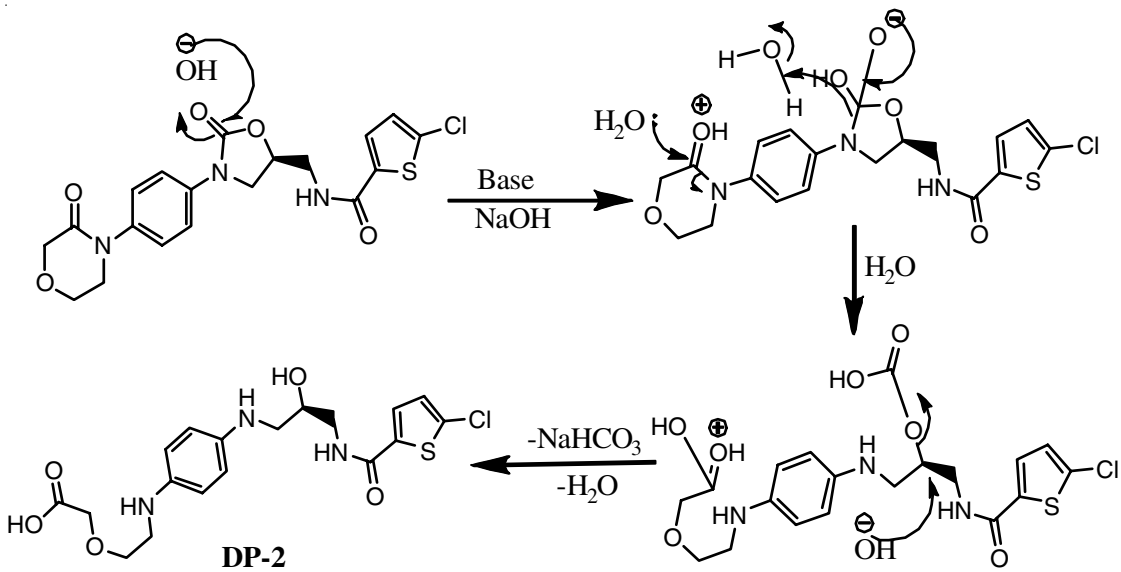

Fig. 6. Possible mechanism of **DP-2** formation

TABLE-3
COMPARATIVE FTIR DATA (cm^{-1}) OF RIVAROXABAN AND DEGRADATION PRODUCTS

API	DP-1	DP-2	DP-3	DP-4	Region (cm^{-1})	Assignment
~3354	~3386, 3332	~3359	~3743, 3442	~3744, 3377	3700-3300	O-H/N–H stretching
~3073, 3022, 2976	~3091	~3088	–	~2941	3200-3000	C–H alkene stretching
~2937	~2901	~2926	–	~2887, 2838	2840-3000	C–H aliphatic stretching
~1741, 1666, 1643	~1745, 1717, 1633	~1735, 1644	~1699	~1631	1680-1630	C=O stretching
~1549, 1515, 1429	~1558, 1519, 1429	~1516, 1425	~1427, 1382	~1517, 1460, 1426	1600-1450	C-H Bending
~1121, 1143, 1215	~1145	~1323, 1226	-	~1322, 1259	1350-1000	C–N stretching
~827, 749	~813, 754	~814, 740	~756	~802, 740	850-500	C–Cl/C-S stretching

signal indicates the presence of acid group, stretching frequency at 1699 cm^{-1} indicates the presence of keto group, stretching frequency at 756 cm^{-1} indicates the presence of sulphur group. From FT-IR, major frequencies confirmed the presence of acid, sulphur and keto functional groups is shown in Table-3.

Degradation product-4: The **DP-4** gave protonated molecular ion 452.0687(M-H) with 2.0680 ppm error in HRMS with respect to molecular formula of $C_{19}H_{19}N_3O_6ClS$ (Fig. 2e) and the chemical shifts of degradation products are given in Table-2. A significant measurable chemical shift for 3-morpholinone ring is seen in proton NMR of **DP-4**. The chemical shift of methylene group (-CH_2-) has shifted 0.5 ppm up field from 3.71 to 3.17 ppm and also in ^{13}C NMR the same methylene carbon has shifted up field 6.14 ppm from 48.99 to 42.85 ppm. The amidic carbonyl carbon of 3-morpholinone ring shifted to downfield nearly 5.8ppm from 165.94 to 171.81 ppm, and in HMBC data, no correlation was observed for the methylene group (-CH_2-) protons with the same amidic carbonyl carbon (C_6). This suggests that 3-morpholinone ring has opened and formed substituted 2-(2-aminoethoxy) acetic acid as shown in Fig. 7. The FTIR stretching frequency at 3744 and 3377 cm^{-1} with broad signal indicates the presence of acid group and NH group, stretching frequency at 1631cm^{-1} indicates the presence of keto or amide group, stretching frequency at 802 and 740 cm^{-1} indicates the presence of chloro and sulphur group. The major frequencies confirmed the presence of acid, alcohol, amide, amine, sulphur and keto functional groups shown in

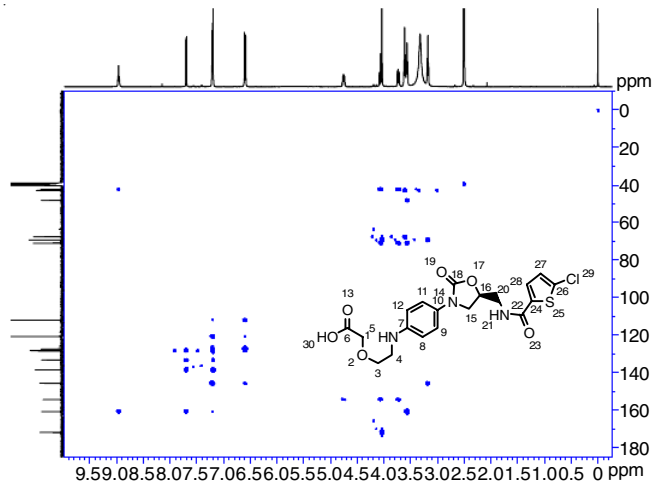

Fig. 7. NMR-HMBC spectra of rivaroxaban **DP-4**

Table-3. The possible mechanism of **DP-4** formation from API through acid degradation is shown in Fig. 8.

Conclusion

The forced degradation behaviour of rivaroxaban was studied as per ICH prescribed guidelines. The drug was subjected to acid, base, oxidative, thermal and photolytic stress conditions. Four degradation products were formed under stress conditions. All the products were selectively isolated and fully characterized using various 1D-2D NMR and mass spectro-

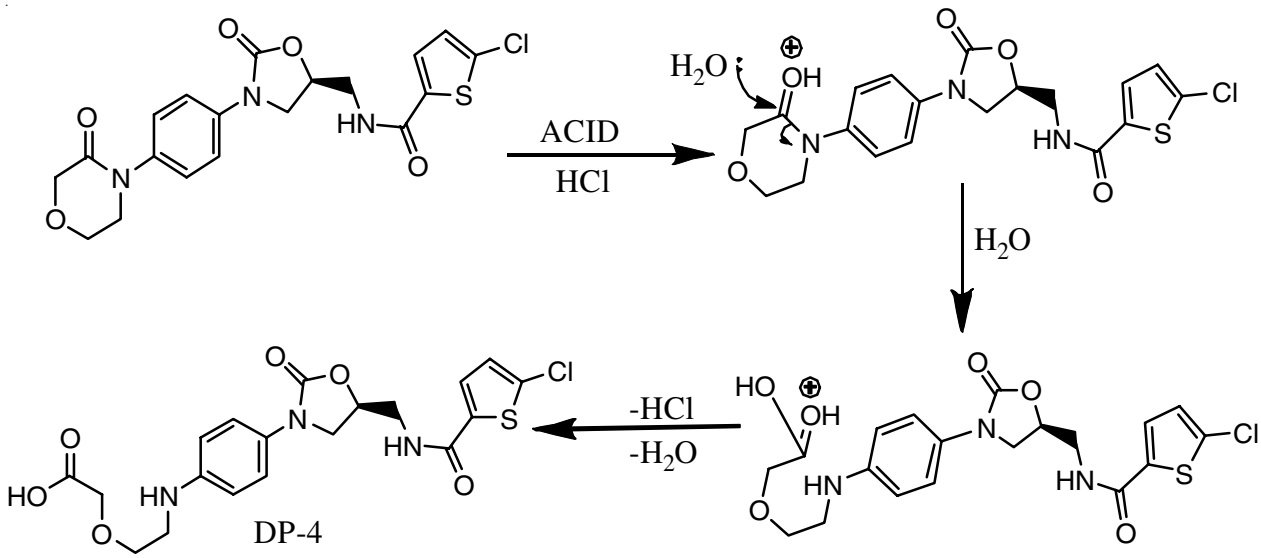

Fig. 8. Possible mechanism of **DP-4** formation

scopic techniques. The **DP-1** and **DP-4** matched with the reported degradants with the reported data [22] and **DP-2** and **DP-3** were identified as the novel impurities with full structural characterization.

ACKNOWLEDGEMENTS

The authors thank the Management of GVK Biosciences Pvt. Ltd., Hyderabad, India for supporting this work.

CONFLICT OF INTEREST

The authors declare that there is no conflict of interests regarding the publication of this article.

REFERENCES

1. E. Kesieme, C. Kesieme, N. Jebbin, E. Irekpita and A. Dongo, *J. Blood Med.*, **2**, 59 (2011); https://doi.org/10.2147/JBM.S19009
2. S. Roehrig, A. Straub, J. Pohlmann, T. Lampe, J. Pernerstorfer, K.H. Schlemmer, P. Reinemer and E. Perzborn, *J. Med. Chem.*, **48**, 5900 (2005); https://doi.org/10.1021/jm050101d
3. A.G. Turpie, *Eur. Heart J.*, **29**, 155 (2007); https://doi.org/10.1093/eurheartj/ehm575
4. T. Chen and S. Lam, *Cardiol. Rev.*, **17**, 192 (2009); https://doi.org/10.1097/CRD.0b013e3181aa2154
5. C.B. Burness and C.M. Perry, *Drugs*, **74**, 243 (2014); https://doi.org/10.1007/s40265-013-0174-4
6. N.J. Carter and G.L. Plosker, *Drugs*, **73**, 715 (2013); https://doi.org/10.1007/s40265-013-0056-9
7. K. Kiser, Oral Anticoagulation Therapy: Cases and Clinical Correlation, Springer, p. 11 (2017).
8. E. Perzborn, S. Roehrig, A. Straub, D. Kubitza and F. Misselwitz, *Nat. Rev. Drug Discov.*, **10**, 61 (2011); https://doi.org/10.1038/nrd3185
9. A.K. Singh, V. Noronha, A. Gupta, D. Singh, P. Singh, A. Singh and A. Singh, *Cancer Res. Stat. Treat.*, **3**, 264 (2020); https://doi.org/10.4103/CRST.CRST_122_19
10. T.A. Fattah and A. Saeed, *Tetrahedron: Asym.*, **28**, 485 (2017); https://doi.org/10.1016/j.tetasy.2017.02.010
11. F. Iram, M.A. Iqbal and A. Husain, *Int. J. Pharma Chem. Res.*, **1**, 140 (2015).
12. W. Mueck, J. Stampfuss, D. Kubitza and M. Becka, *Clin. Pharmacokinet.*, **53**, 1 (2014); https://doi.org/10.1007/s40262-013-0100-7
13. R. Burghaus, K. Coboeken, T. Gaub, L. Kuepfer, A. Sensse, H.-U. Siegmund, W. Weiss, W. Mueck and J. Lippert, *PLoS ONE*, **6**, e17626 (2011); https://doi.org/10.1371/journal.pone.0017626
14. E. Perzborn, S. Roehrig, A. Straub, D. Kubitza, W. Mueck and V. Laux, *Arterioscler. Thromb. Vasc. Biol.*, **30**, 376 (2010); https://doi.org/10.1161/ATVBAHA.110.202978
15. B.I. Eriksson, L.C. Borris, O.E. Dahl, S. Haas, M.V. Huisman, A.K. Kakkar, E. Muehlhofer, C. Dierig, F. Misselwitz and P. Kälebo, *Circulation*, **114**, 2374 (2006); https://doi.org/10.1161/CIRCULATIONAHA.106.642074
16. European Medicines Agency, CHP Assessment Report for Xarelto (EMEA/543519/2008)" (PDF). Retrieved 2009-06-11 (2008).
17. M. Çelebier, T. Reçber, E. Koçak and S. Altinö, *Braz. J. Pharm. Sci.*, **49**, 359 (2013).
18. M. Çelebier, T. Reçber, E. Koçak, S. Altinö and S. Kir, *J. Chromatogr. Sci.*, **54**, 216 (2016); https://doi.org/10.1093/chromsci/bmv135
19. P.B.M. Derogis, L.R. Sanches, V.F. de Aranda, M.P. Colombini, C.L.P. Mangueira, M. Katz, A.C.L. Faulhaber, C.E.A. Mendes, C.E. dos Santos Ferreira, C.N. França and J.C. de Campos Guerra, *PLoS ONE*, **12**, e0171272 (2017); https://doi.org/10.1371/journal.pone.0171272
20. A. Varga, R.C. Serban, D.L. Muntean, C.M. Tatar, L. Farczadi and I. Tilea, *Rev. Roman. Med. Lab.*, **25**, 145 (2017); https://doi.org/10.1515/rrlm-2017-0007
21. A.K. Pinaz and K.S. Muralikrishna, *Asian J. Pharm. Anal.*, **3**, 62 (2013).
22. N.R. Ramisetti and R. Kuntamukkala, *RSC Adv.*, **4**, 23155 (2014); https://doi.org/10.1039/c4ra00744a
23. C. Weinz, T. Schwarz, D. Kubitza, W. Mueck and D. Lang, *Drug Metab. Dispos.*, **37**, 1056 (2009); https://doi.org/10.1124/dmd.108.025569
24. D. Lang, C. Freudenberger and C. Weinz, *Drug Metab. Dispos.*, **37**, 1046 (2009); https://doi.org/10.1124/dmd.108.025551
25. G. Rohde, *J. Chromatogr. B Analyt. Technol. Biomed. Life Sci.*, **872**, 43 (2008); https://doi.org/10.1016/j.jchromb.2008.07.015
26. International Conference on Harmonization (ICH): Q1A(R2) Stability Testing of New Drug Substances and Products, (2003).
27. International Conference on Harmonization (ICH): Q3B(R2) Impurities in New Drug Products (2006).
28. WHO, Draft Stability Testing of Active Pharmaceutical Ingredients and Pharmaceutical Products, World Health Organization: Geneva (2007).
29. FDA, Guidance for Industry: Stability Testing of Drug Substances and Drug Products (Draft Guidance). Food and Drug Administration, Rockville, MD (1998).